Structural Engineering and Mechanics, Vol. 16, No. 5 (2003) 581-595

DOI: http://dx.doi.org/10.12989/sem.2003.16.5.581

A two-step approach for joint damage diagnosis of framed structures using artificial neural networks

W. L. Qu† and W. Chen‡

College of Civil Engineering and Architecture, Wuhan University of Technology Wuhan 430070, P.R. China

Y. Q. Xiao‡†

Department of Building and Construction, City University of Hong Kong, Kowloon, Hong Kong

(Received December 23, 2002, Accepted August 6, 2003)

Abstract. Since the conventional direct approaches are hard to be applied for damage diagnosis of complex large-scale structures, a two-step approach for diagnosing the joint damage of framed structures is presented in this paper by using artificial neural networks. The first step is to judge the damaged areas of a structure, which is divided into several sub-areas, using probabilistic neural networks with natural Frequencies Shift Ratio inputs. The next step is to diagnose the exact damage locations and extents by using the Radial Basis Function (RBF) neural network with the second Element End Strain Mode of the damaged sub-area input. The results of numerical simulation show that the proposed approach could diagnose the joint damage of framed structures induced by earthquake action effectively and has reliable anti-jamming abilities.

Key words: framed structures; joint damage; damage diagnosis; element end strain mode; artificial neural network.

1. Introduction

During the service life of most engineering structures, variant damages may occur due to the different environmental perturbations and/or excessive loads. These damaged structures may not meet their intended services and could possibly end in partial or total collapses (Li 2001a, 2002b, 2003). Therefore, it would be necessary to diagnose the damages inside a structure during its service life, especially after earthquakes or fires.

Framed structures are widely used in civil engineering. Research works on damage diagnosis of framed structures have been conducted during the last three decades (Cawley and Adams 1979, Heam 1991, Yun *et al*. 2001, Zhou and Shen 1997, Lu 1997). However, most of these researches are mainly concerned with element damages, partly because it is convenient to establish the Finite Element Model of a structure with element damages, and easy to validate the damage diagnosis in

† Professor
‡ Research Student
‡† Research Fellow

experiments. However, the beam-to-column connections (joints) of framed structure are more likely to suffer damages, as indicated in site investigations and experiments, especially for steel framed structures. The joint damages may take place in steel frames due to bolt hole crack, bolt failure, weld joints failure and plastic deformation of connective components. The joints of RC frames will behave like plastic joints under strong seismic impact (Li *et al*. 1999, Wu and Li 2003), which may result in joint damages. Therefore, it is necessary to develop an efficient approach for joint damage diagnosis for framed structures.

Recently, the damage-diagnosing approaches based on inversed structural dynamic analysis became the majority of the researches in the field of structural health monitoring (Rizos *et al*. 1990, Liang *et al*. 1992, Li 2002a, 2001b, 2001c). Most of these approaches diagnose the structural damages directly, and showed competent efficiency on simple structures (Rizos *et al*. 1990, Liang *et al*. 1992, Qian *et al*. 1990, Ostachowicz and Krawczuk 1991). However, these approaches are hard to be applied to complex large-scale structures. There are mainly two reasons for that:

(1) No matter which approach is adopted, the total computing amount is enormous and even impracticable for current computers because the complex large-scale structures are composed of numerous elements and have too many Degrees of Freedom.

(2) In general, experimental measurements can provide reliable but limited information (i.e., modal parameters of several modes). Therefore, the incompleteness of the measurements becomes the main obstacle in the damage diagnosis. In other words, how to apply the damage-diagnosing approaches to complex large-scale structures is still under investigation.

Two-step approaches were presented recently for damage detection (Li *et al.* 1998b, Kim *et al.* 1993). Li *et al.* (1998b) had developed a two-step damage-diagnosing approach for framed structures. The first step is to determine the stiffness matrix for lateral floor displacements and related mode shapes by identifying the eigenvalues of the matrix with a certain bandwidth. The second step is to identify the damages of the beams and columns by using the linear programming method based on the results of the first step. Kim *et al.* (1993) developed a two-step damage-diagnosing method based on the incomplete measurements. The first step is to judge the damaged area of a structure using the model updating technique. The second step is to diagnose the damage locations and extents from the sensitivity analysis of structural damages.

A two-step approach for damage diagnosis of framed structures using artificial neural networks is presented in this paper. The first step is to divide a structure into several sub-areas and to judge the damaged areas of the structure using probabilistic neural networks with the first several natural Frequencies Shift Ratio (FSR) inputs. The next step is to diagnose the exact damage locations and extents using the RBF neural networks with the second Element End Strain Mode (EESM) of the damaged sub-area input. The efficiency of the proposed approach is illustrated through a numerical simulation for a 10-story framed structure. The numerical results show that the proposed approach could successfully diagnose the joint damages of the framed structure induced by earthquake action, even with limited measurement information. The method is proved to also have good anti-jamming abilities.

2. Two-step approach for damage diagnosis of framed structures

2.1 Damage diagnosis process

In general, the conventional direct damage-diagnosing methods are difficult to be applied to complex large-scale structures due to the incompleteness of measurements. Therefore, if the damaged sub-areas can be determined inchoately, and the damage is diagnosed just inside the range of the sub-area based on the achievement of the anterior step, the total amount of measurements required will be greatly reduced. The diagnosis results will be more reliable. Therefore, this approach could be used for diagnosing not only damages of simple small-scale structures but also damages of complex large-scale structures.

The proposed approach is composed of two steps:

(1) Damaged sub-area ascertainment

The structure is divided into several sub-areas according to its characteristics. The relationship between the first several Frequency Shift Ratios (FSR), which is calculated from the damaged structure and the intact structure, and the locations of the damaged sub-areas are transmitted into the probabilistic neural networks (PNN) to establish a system for initial damage diagnosis. And based on the established system, the locations of the damaged sub-area can be ascertained (Fig. 1).

(2) Exact damage diagnosis in the sub-areas

The shift of the Element End Mode Strain (EESM) between the damaged structure and the intact structure in the damaged sub-areas identified by the first step is determined. The relationship between the shift and the exact damage locations and extents are transmitted into the Radial Basis Functions (RBF) networks. Then, the system for the exact damaged diagnosis is established (Fig. 2).

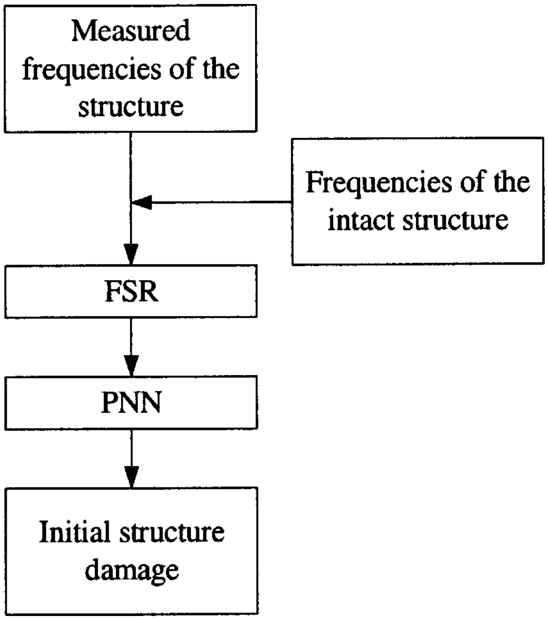

Fig. 1 Damaged sub-area ascertainment system

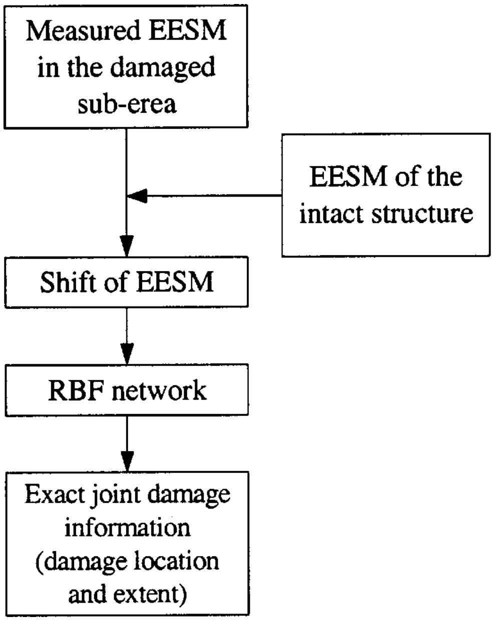

Fig. 2 Exact joint damage diagnosis system

2.2 Damaged sub-area ascertainment system using PNN

2.2.1 Damaged sub-area ascertainment based on FSR

Experimental researches (Li *et al*. 1994, 1998a) showed that the measurement of natural frequency is the most accurate among structural dynamic characteristics. If the damage locations could be estimated approximately using the first several natural frequencies, the damage diagnosis will just be limited inside the known areas, and the direct conventional approaches could be applied to diagnose the exact damage locations and extents, which would greatly reduce the total amount of measurements required.

Cawley and Adams (1979) had reported that when damages took place in a structure, discretional two frequencies shift ratio ($\delta\omega_i / \delta\omega_j,\ i \neq j$) was related with the damage locations rather than the damage extents. Therefore the damage locations can be determined by natural frequencies. Heam (1991) had developed an approach for identifying damage locations using the frequency shift square ratio ($\delta\omega_i^2 / \delta\omega_j^2,\ i \neq j$) of the damaged structure and the intact structure. However, this method would not be valid for symmetrical structures. The damages with the same extent in the symmetrical location would make the frequencies shift in the same trend, which means the frequency-based damage diagnosis approaches would fail in this situation. If the structure is initially divided into several sub-areas according to its characteristics and each sub-area contains several elements, the problem would be simplified. For example, the symmetric structure could be divided into sub-areas, which contain elements in the symmetric locations. Then, the locations of the damaged sub-areas can be determined by FSR. The first several FSR can be calculated as follows:

$$FSR_i = \frac{\omega_{d,i} - \omega_{s,i}}{\omega_{d,1} - \omega_{s,1}} \qquad (i = 1, 2, 3, \ldots) \tag{1}$$

where $\omega_{d,i}$ is the i-th natural frequency of the damaged structure, and $\omega_{s,i}$ is the i-th natural frequency of the intact structure. Then the PNN is introduced to determine the sub-area locations.

2.2.2 Probabilistic neural networks

How to determine structural damaged sub-areas is a problem of pattern classification/recognition. It has been recognized that the PNN is an efficient pattern classification tool (Liang *et al*. 1992), which can work with noise stained data. Specht (1990) first presented the PNN model in 1990. The model is based on probability statistics and Bayes classification criteria. As a pattern recognition tool, the Bayes criterion is an optimum decisive criterion with minimum “expected risk”. It can deal with classification problems with enormous patterns. The PNN presented by Specht (1990) can be modeled with 4 layers, as shown in Fig. 3. When the PNN is to be trained, the networks just simply store the training patterns with no modification, and only the slick factor of the Gauss function is estimated empirically. When the networks are working, the tested pattern “X” is transmitted from the input layer to all the classification units in each pattern layer, where the dot product of pattern “X” and pattern “W” is calculated. Then the dot product is processed in the unit nonlinearly and is transmitted into the summation layer. The units in the summation layer are just connected with relevant pattern units, and estimate probability of each classification. In the decision layer, the tested pattern “X” is divided into the class with maximum posterior probability based on Bayes classification criterion according to its probability estimation.

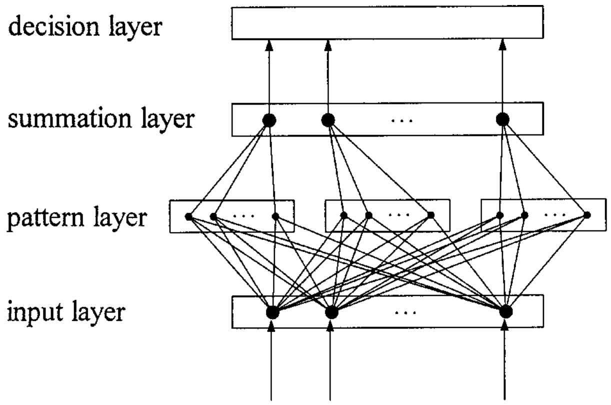

Fig. 3 Layer structure of PNN

Compared with the BP networks, the PNN has some obvious advantages:

(1) The process is simple; the networks always quickly converge to the Bayes optimum solution with good stability.

(2) Training of the PNN does not need too many patterns, and the trained PNN has good pattern classification ability.

(3) The PNN has good pattern appending ability and is tolerant with certain wrong patterns.

2.3 Exact damage diagnosis system using RBF networks

2.3.1 Damage diagnosis of framed structures based on EESM

Most researches on damaged diagnosis utilized the dynamic characteristics of structures such as natural frequencies and mode shapes as damage indicators. However, such studies (Li 2002a, 2001b, 2001c) had proved that the natural frequencies are not sensitive to the damage extents, the damages occurred in different locations and with different extents can cause natural frequencies shift in the same way. Furthermore, the mode shapes are not sensitive to local damage too. The measurement of mode shape is constantly stained by great errors and is often incomplete, which may influence the results of the diagnosis.

As one of structural dynamic characteristics, strain modes have a lot of advantages in this case compared with other dynamic characteristics. Some of these advantages include good measurement precision, low cost, excellent sensibility to local changes, etc. Therefore, strain mode is a proper damage indicator for engineering application. Mode shapes represent generalized orthogonal structural displacements, while structural strain is the derivative of structural displacement. Therefore, a particular strain distribution can be deduced from one mode shape, and this distribution is called strain mode. When damages take place in some local areas of structures, there would be a phenomenon named “stress concentration”, which means that the stress near the damage zone will shift (increase for positive stress or reduce for negative ones) rapidly. According to the Saint-Venant principle, the strain shift in locations far from the damaged area will be much less than that in the damaged area. Therefore, the local damages can be detected since the strain is sensitive to the local change in structure only. The static strain distribution is related to loads acting on the structure, and

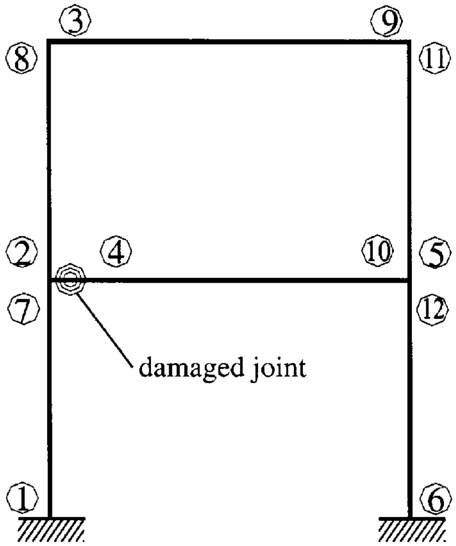

Fig. 4 2-story frame and sequence number of each element end

it would change with the loads shifting. Therefore, the static strain distribution cannot be used as the damage indicator. The strain mode is one of inherent dynamic characteristics of a structure and would not be influenced by loads. If the strain mode of a structure can be obtained before and after damage taking place, it is possible to diagnose the damage locations and extents.

The efficiency of the strain mode as a damage indicator is shown in the following simulation. The structure under consideration is a 2-story frame shown in Fig. 4 and the damage is expected to take place at the joints. If the joint damage is concerned, the Element End Strain Mode (EESM) is used as a damage indicator. The EESM is defined as the particular strain distribution at the ends of each elements of the structure corresponding to each mode shape. Since the strain at each end is arduous, almost impossible to measure, the strain at a certain point near the end is adopted. The distance between the end and the point is empirically determined; twice of the element height is used in the example.

The shift of structural EESM can be calculated from

$$\{v_j\} = \{\psi\}_{d,j} - \{\psi\}_{s,j} \tag{2}$$

where $\{\psi\}_{d,j}$ is the j-th EESM of the damaged structure, and $\{\psi\}_{s,j}$ is the j-th EESM of the intact structure.

It is assumed that joint damage takes place with different extents, such as 10%, 40%, 70% and 90% respectively, at the left end of the beam in the first story of the frame shown in Fig. 4. The first EESM shift $\{v_1\}$ of the frame is shown in Fig. 5. It is obvious that the EESM shift is closely related to joint damage. The location of the damage is just the joint with the maximal EESM shift when only one joint was damaged. When several joints are damaged at the same time, their EESM shifts will interlace with each other. Therefore, it is impossible to determine the damage locations directly just by the EESM shift. The neural networks are introduced to deal with this problem.

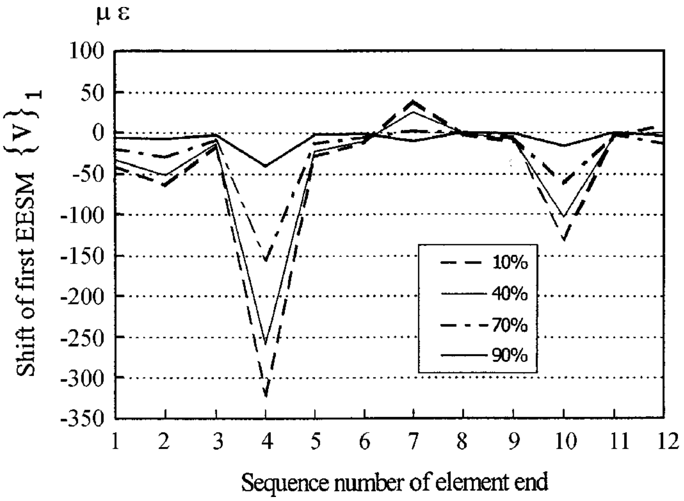

Fig. 5 Shift of the first element end strain mode

2.3.2 RBF networks

Since the EESM shift is closely related to joint damage, the joint damage can be diagnosed using the EESM shift of a structure if the relationship can be mapped. BP network is widely used in various areas for its mapping abilities. But there are still some unavoidable defects of BP network:

(1) The convergence process is so slow that the computation will take a long time.

(2) The convergence will drop into local minimum, instead of global one.

(3) There is no unified principle for determining scale of the BP networks, which is conventionally achieved by experiences.

A series of other ANN, such as RBF networks, have shown their superiority in damage detection researches. A radial basis function (RBF) neural network is usually trained to map a vector $x_k \in R^m$ into a vector $y_k \in R^n$ where the pairs (x_k, y_k), $1 \le k \le M$ form the training set. If this mapping is viewed as a function in the input space R^m, learning can be seen as a function approximation problem. From this point of view, learning is equivalent to finding a surface in a multidimensional space that provides the best fit for the training data. Generalization is therefore synonymous with interpolation between the data points along the constrained surface generated by the fitting procedure as the optimum approximation to this mapping. The performance of a RBF neural network depends on the number and positions of the radial basis functions, their shapes, and the method used for learning the input-output mapping. The existing learning strategies for RBF neural networks can be classified as follows:

(1) Strategy selects radial basis function centers randomly from the training data.

(2) Strategy employs unsupervised procedures for selecting radial basis function centers.

(3) Strategy employs supervised procedures for selecting radial basis function centers.

A hybrid learning process for training RBF neural networks with Gaussian radial basis functions is widely used in practice. The structure of a typical RBF network is shown in Fig. 6.

Therefore, if the damaged sub-area can be determined in the prior step, the exact damage can be diagnosed using the RBF networks with several first EESM shifts of the structure.

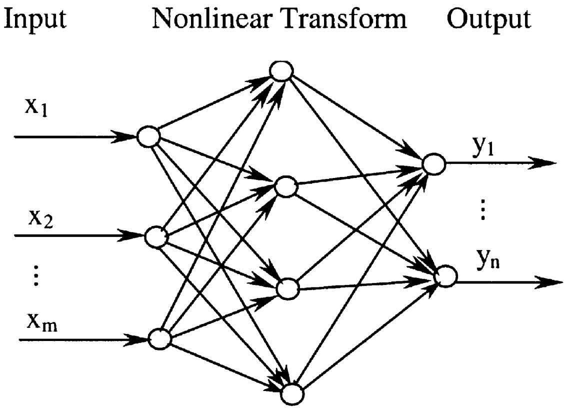

Fig. 6 Structure of RBF network

3. Key techniques in the two-step damage diagnosis system

3.1 Finite element model of a structure with joint damage

The conventional procedures for structural analysis usually assume that joints are pinned or completely rigid. However, most joints of structures in reality are semi-rigid. The joint behavior makes an important contribution to the behavior of the whole structure, and the performance of the joints is one of the critical factors in structural collapses (Li and Chen 2003). Among the various possible deformation modes for the semi-rigid connections, the most important mode is the rotational deformation caused by a bending moment. The basic description of the flexural behavior is its moment-rotation relationship, which may be represented as the joint flexural rigidity. The joint damage may be quantified by the reduction of the connection rigidity. If the rotational stiffness of the joint can be evaluated before and after the damage, the damage severity can be determined based on the shift of stiffness. In this study, a frame element with incorporating joint flexural rigidity is modeled. Then the joint damage severities are identified based on the changes in the modal properties using the neural networks. The semi-rigid connection is modeled as zero-length rotational springs at the ends of a beam, as shown in Fig. 7. The rotational stiffness is infinite for the spring of the rigid joints and zero for that of pinned joints. Yun *et al*. (2001) has presented a particular joint fixity factor. The joint fixity factor can be defined using the rotational stiffness (k_{r1}, k_{r2}) of the spring as follows

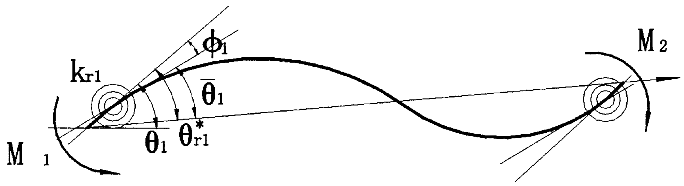

Fig. 7 Model of semi-connected elements

$$\gamma_1 = \frac{1}{1 + \dfrac{3EI/L}{k_{r1}}} \qquad \gamma_2 = \frac{1}{1 + \dfrac{3EI/L}{k_{r2}}} \tag{3}$$

where EI/L is the stiffness of the beam. Then the joint fixity factor can be used to describe the beam-column connections. As proved in the previous study (Yun *et al.* 2001), for the pinned joints, $0 \le \gamma < 0.143$, for the rigid joints, $0.891 \le \gamma \le 1$, and for the semi-connected joints, $0.143 \le \gamma < 0.891$.

The stiffness matrix of a beam element with semi-rigid connections at ends is

$$[k] = \begin{bmatrix} \frac{EA}{L} & & & & & \\ 0 & \frac{12EI}{L^3}\left(\frac{f_1}{f_7}\right) & & & \textit{symmetric} & \\ 0 & \frac{6EI}{L^2}\left(\frac{f_2}{f_7}\right) & \frac{4EI}{L}\left(\frac{f_3}{f_7}\right) & & & \\ \frac{-EA}{L} & 0 & 0 & \frac{EA}{L} & & \\ 0 & -\frac{12EI}{L^3}\left(\frac{f_1}{f_7}\right) & -\frac{6EI}{L^2}\left(\frac{f_2}{f_7}\right) & 0 & \frac{12EI}{L^3}\left(\frac{f_1}{f_7}\right) & \\ 0 & \frac{6EI}{L^2}\left(\frac{f_6}{f_7}\right) & \frac{2EI}{L}\left(\frac{f_5}{f_7}\right) & 0 & -\frac{6EI}{L^2}\left(\frac{f_6}{f_7}\right) & \frac{4EI}{L}\left(\frac{f_4}{f_7}\right) \end{bmatrix} \tag{4}$$

where $f_1 = \gamma_1 + \gamma_2 + \gamma_1\gamma_2$, $f_2 = \gamma_1(2+\gamma_2)$, $f_3 = 3\gamma_1$, $f_4 = 3\gamma_2$, $f_5 = 3\gamma_1\gamma_2$, $f_6 = \gamma_2(2+\gamma_1)$, $f_7 = 4 - \gamma_1\gamma_2$.

When $\gamma_1 = \gamma_2 = 1$, Eq. (4) is the stiffness matrix of beam elements in a framed structure. The Finite Element Model of framed structures can be established by using the stiffness matrix of semi-connected beam elements. Thus the dynamic characteristics of damaged structures with different damage locations and severities can be calculated.

3.2 Noise injection training of ANN

Measurements from a structure, such as acceleration and dynamic strain are possibly affected by noise. To reduce the noise effects and promote the precision of the diagnosis results, the ANN can be trained with noise injection methods, which means that the input patterns can be processed considering the noise effects as

$$\tilde{\phi}_k = \phi_k(1 + \beta_k) \tag{5}$$

where ϕ_k and $\tilde{\phi}_k$ are the (calculated) exact and the noise-injected patterns respectively, and β_k is the zero mean Gaussian random noise with constraint of $|\beta_k| \le 1$. For different patterns, the noise effects are regarded as being independent each other and thus different β_k is taken into account. The root-mean-square of β_k is relatively small for the natural frequency patterns, since the measurement is relatively reliable. The root-mean-square of β_k may be larger for the strain mode patterns considering the error of measurements.

3.3 Evaluation of the diagnosis results

To evaluate the diagnosis results, the Mean Extent Error (MEE) and the Mean Location Error (MLE) are adopted in this study. The MEE is the average of the absolute estimation error of all the joint damage extent (joint fixity factor):

$$MEE = \frac{1}{NE}\sum_{i=1}^{NE}|\gamma_{d,i} - \gamma_{e,i}| \tag{6}$$

where NE is the number of the joints of the whole structure, $\gamma_{d,i}$ is the joint fixity factor estimated by ANN, and $\gamma_{e,i}$ is the exact joint fixity factor.

The MLE is used to evaluate the locations of the damaged sub-area, defined as

$$MLE = \frac{1}{NS}\sum_{i=1}^{NS}\xi_1; \qquad 0 \le MLE \le 1 \tag{7}$$

where NS is total number of the sub-areas into which the structure is divided, ξ_i is the location error for the i-th sub-area. $\xi_i = 0$ for the case of the damage occurs in this sub-area and $\xi_i = 1$ otherwise.

4. Experimental measurement of EESM

The experiment measurement of EESM can be obtained (Zhou and Shen 1997) using resonance excitation method. The strain response of a framed structure is

$$\{\varepsilon\} = \sum_{r=1}^{m}\frac{\{\psi_r^{\varepsilon}\}\{\varphi_r\}^T\{F\}}{k_r - \omega^2 m_r + j\omega c_r}e^{jwt} \tag{8}$$

where ψ_r^{ε} is the r-th strain mode, φ_r is the r-th mode shape of displacement, k_r, m_r, c_r are the modal stiffness, modal mass and modal damping, respectively; $\{F\}$ is amplitude vector of harmonic excitations applied at the stories of the frame.

The strain transfer function at the i-th element end caused by the unit harmonic excitation at the j-th story is

$$H_{ij}^{\varepsilon} = \sum_{r=1}^{m}\frac{\psi_{ir}^{\varepsilon}\varphi_{jr}}{k_r - \omega^2 m_r + j\omega c_r} = \sum_{r=1}^{m}\frac{\psi_{ir}^{\varepsilon}\varphi_{jr}/k_r}{1 - \left[\frac{\omega}{\omega_r}\right]^2 + \frac{2j\xi_r\omega}{\omega_r}} \tag{9}$$

where $\xi_r = \frac{c_r}{2\sqrt{m_r k_r}}$ and $\omega_r = \sqrt{\frac{k_r}{m_r}}$ are the r-th modal damping ratio and the r-th natural frequency of the structure, respectively.

When the frequency of the excitation applied at the j-th story equals to a natural frequency of the structure, for example the natural frequency of the s-th mode, Eq. (9) can be rewritten as

$$H_{ij}^{\varepsilon} = \frac{\psi_{js}^{\varepsilon}\varphi_{js}}{2j\xi_s k_s} + \sum_{\substack{r=1 \\ r \neq s}}^{m} \frac{\psi_{ir}^{\varepsilon}\varphi_{jr}/k_r}{1 - \left[\frac{\omega}{\omega_r}\right]^2 + \frac{2j\xi_r\omega}{\omega_r}} \tag{10}$$

Since the modes of a framed structure are usually not closely spaced, the s-th mode contributes mainly in H_{ij}^{ε}, while contributions of other modes ($r \neq s$) can be ignored. Thus, Eq. (10) can be rewritten approximately as

$$H_{ij}^{\varepsilon} = \frac{\psi_{js}^{\varepsilon}\varphi_{js}}{2j\xi_s k_s} \tag{11}$$

Thus, we have

$$\{\psi\}_{js}^{\varepsilon} = \frac{2j\xi_s k_s}{\varphi_{js}F_j(\omega_s)} \cdot \varepsilon_j(\omega_s) \tag{12}$$

where $\varepsilon_j(\omega_s)$ is the strain amplitude at the j-th story.

When the frame is excited at the j-th story with the s-th frequency ω_s, $F_j(\omega_s)$ is invariable, the modal parameters ξ_s, k_s and φ_{js} are all constants too. Then a factor α is defined accordingly as

$$\alpha = \frac{2j\xi_s k_s}{\varphi_{js}F_j(\omega_s)} \tag{13}$$

where α is constant. Then

$$\psi_{js}^{\varepsilon} = \alpha\varepsilon_j(\omega_s) \tag{14}$$

Based on the formulas presented above, it is found that the s-th EESM $\{\psi^{\varepsilon}\}_s$ can be obtained when the framed structure is subjected to the loads with the s-th resonance frequency and the amplitude vectors of strain response at certain points near the ends of the elements are measured.

5. Numerical simulation

5.1 Example structure

To investigate the effectiveness the proposed two-step approach for joint damage diagnosis of framed structures using ANN, a 10-story frame structure shown in Fig. 8 is considered for joint damage diagnosis by numerical simulation. The length of each span L of the frame is 4.0 m, height of each story is 3.0 m, and other parameters of the frame are shown in Table 1. The frame is divided into 5 sub-areas, and all the sub-areas are marked in Fig. 8. The first two mode shapes of the structure are shown in Fig. 9. To simplify the simulation, the joints damages are assumed to take place just at the end of the beams.

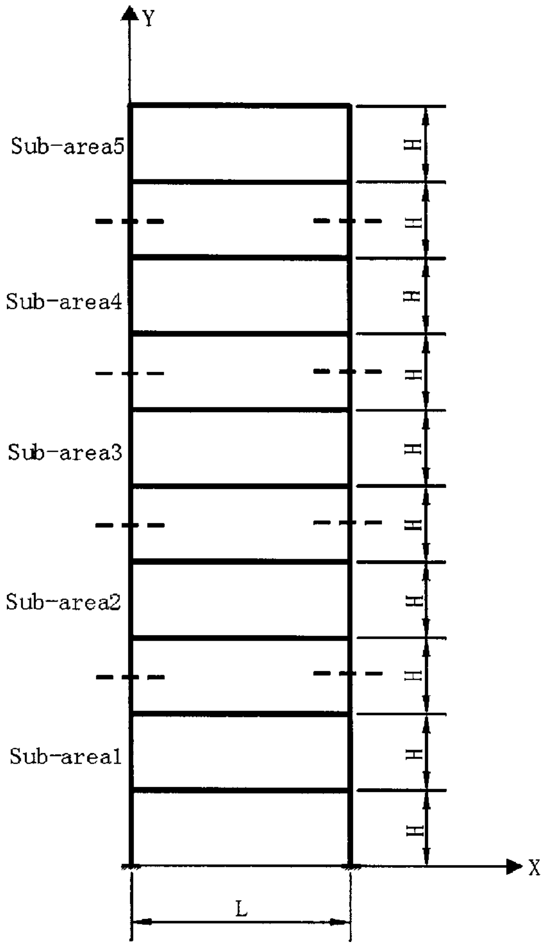

Fig. 8 10-Story frame and sub-area marks

Table 1 Parameters of the frame

Element type	b(m)	h(m)	A(m^2)	I(m^4)	E(pa)	ρ(kg/m^3)
Column	0.4	0.4	1.6×10^{-1}	2.13×10^{-3}	2.05×10^{10}	2500
Beam	0.25	0.3	7.5×10^{-2}	5.62×10^{-4}		

5.2 Training of the ANN

There are two cases considered in the training of ANN for the purpose of simplification. The first case assumes that damage appears in one sub-area and the second case considers that damages occur in two sub-areas. In the second case it is assumed only one joint damage will take place in each sub-area. The severity of joint damage is described by $\alpha(\alpha = 1-\gamma,\ \alpha = 0.1, 0.2, \ldots, 0.9)$. For the example structure, 15570 training patterns for the ANN are acquired according to different

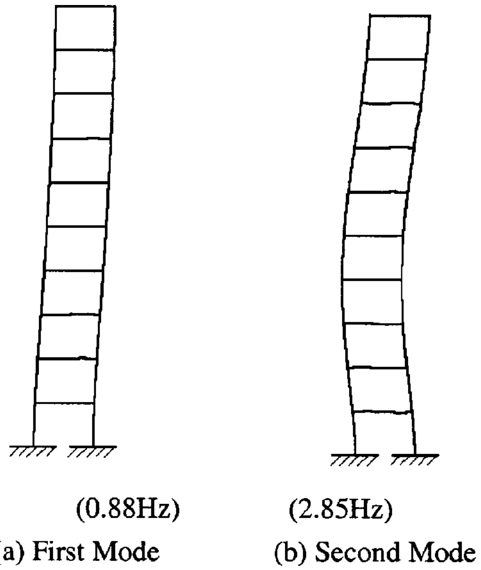

Fig. 9 The first two mode shapes of the frame

damage severities and locations. The training patterns consist of neural FSR patterns and EESM shift patterns. To measure the respective effects of different inputs on the diagnosis results of the ANN, the following two inputs of EESM shift for RBF networks are taken into account:

(1) The first EESM shift;

(2) The second EESM shift;

10610 patterns are used to train the ANN, and 4960 are used as test patterns for the ANN. The PNN system for identifying the damaged sub-area is acquired after the FSR patterns are input to train the networks. And the RBF networks system for exact damage diagnosis is acquired with EESM shift patterns input. Noise injection training technique is applied to enhance the anti-interference capability of the networks.

5.3 Results of damage diagnosis

4960 test patterns, with different levels of noise added or not, are input into the established systems to evaluate the damage diagnosis capabilities of the proposed approach. The ascertainment results of damaged sub-areas using the PNN systems, which are trained with the noise injection training technique, are listed in Table 2. The results show that the noise injection training technique can greatly enhance the anti-interference capability of the system and reduce the diagnosis errors. Even when the noise level is as low as 10%, the PNN system trained with the noise injection training technique can still detect the damaged sub-areas successfully.

The results of the exact damage diagnosis in the detected sub-areas using the RBF networks system with the first order EESM shift and the second order EESM shift input are shown in Table 3. It can be concluded from the results that using the second EESM shift as the input is superior to the first EESM shift since the former contains more bending information of the structure and can represent the connecting characteristics of the structure more accurately.

Table 2 Results of damaged sub-area ascertainment using PNN (MLE)

ANN	Noise Level (%)		
	1	5	10
PNN trained without noise inject technique	0.02	0.06	0.13
PNN trained with noise inject technique	0.004	0.007	0.013

MLE: Mean Location Error, the smaller of the value indicating the better performance

Table 3 Results of exact damage diagnosis using RBF networks (MEE)

Input of ANN	Noise Level		
	5	10	15
First EESM shift	0.00040	0.00070	0.00110
Second EESM shift	0.00012	0.00025	0.00046

MEE: Mean Extent Error, the smaller of the value indicating the better performance.

6. Conclusions

In this paper, a two-step approach using artificial neural networks for joint damage diagnosis of framed structures is proposed. With the theoretical analysis and numerical simulation some conclusions are summarized as follows

(1) The presented approach is a useful tool in joint damage diagnosis of framed structures. It can reduce the amount of measurements greatly, and has not only good anti-interference capability, but also satisfactory accuracy.

(2) The EESM shift is a good damage indicator for joint damage diagnosis of framed structures. When combined with the RBF networks, the second EESM shift is superior to the first one and can diagnosis the joint damage successfully.

(3) The noise injection technique can enhance the anti-interference capability of the neural networks system greatly, and should be adopted in the implementation of the proposed approach.

References

Cawley, P. and Adams, R.D. (1979), “The location of defects in structures from measurements of natural frequencies”, *Journal of Strain Analysis*, **14**, 49-57.

Heam, G. (1991), “Modal analysis for damage detection in structures”, *J. Struct. Eng.*, ASCE, **117**(10), 3042-3063.

Kim, H., Young, M. and Bartkowicz, T.J. (1993), “Two-step structural damage detection approach with limited instrumentation”, *J. Struct. Eng.*, ASCE, **119**(2), 258-264.

Li, Q.S., Cao, H. and Li, G.Q. (1994), “Analysis of free vibrations of tall buildings”, *J. Eng. Mech.*, ASCE, **120**(9), 1861-1876.

Li, Q.S., Fang, J.Q., Jeary, A.P. and Wong, C.K. (1998a), "Full scale measurements of wind effects on tall buildings", *J. Wind Eng. Ind. Aerod.*, **74-76**, 741-750.

Li, G.Q., Hao, K.C. and Lu, Y. (1998b), "Two step approach for damage identification of framed structures", *Journal of Tongji University*, **26**(5), 483-487.

Li, Q.S., Fang, J.Q. and Jeary, A.P. (1999), "Vibration analysis of tall buildings with narrow rectangular plane configuration", *The Structural Design of Tall Buildings*, **7**(4), 307-322.

Li, Q.S. (2000a), "A computational approach for free vibration of non-uniform flexural-shear plates", *Comput. Method Appl. Mech. Eng.*, **190**, 3-23.

Li, Q.S. (2000b), "Free vibration of elastically restrained flexural-shear plates with varying cross-section", *J. Sound Vib.*, **235**, 63-85.

Li, Q.S. (2001a), "Buckling of multi-step cracked columns with shear deformation", *Eng. Struct.*, **23**(4), 356-364.

Li, Q.S. (2001b), "Dynamic behaviour of multi-step cracked beams with varying cross-section", *J. Acoust. Soc. Am.*, **109**(6), 3072-3075.

Li, Q.S. (2001c), "Vibratory characteristics of multi-step beams with an arbitrary number of cracks and concentrated masses", *Appl. Acoust.*, **62**(6), 691-706.

Li, Q.S. (2001d), "Vibratory characteristics of multi-step non-uniform orthotropic shear plates with line supports and line masses", *J. Acoust. Soc. Am.*, **110**, 1360-1371.

Li, Q.S. (2002a), "An exact approach for free vibration analysis of non-uniform beams with an arbitrary number of cracks and concentrated masses", *J. Sound Vib.*, **252**(3), 509-525.

Li, Q.S. (2002b), "Buckling of an elastically restrained multi-step non-uniform beam with multiple cracks", *Archive of Applied Mechanics*, **72**, 522-535.

Li, Q.S. (2003), "Class of exact solutions for buckling of multi-step non-uniform columns with an arbitrary number of cracks subjected to concentrated and distributed axial loads", *Int. J. Eng. Sci.*, **41**, 569-586.

Li, Q.S. and Chen, J.M. (2003), "Nonlinear elastoplastic dynamic analysis of single-layer reticulated shells subjected to earthquake excitation", *Comput. Struct.*, *An Int. J.*, **81**, 177-188.

Lu, Q.H. (1997), "Neural networks methods in detection of structural modification and damage based on strain mode theory", PhD Dissertation, Tsinghua University.

Liang, R.H., Hu, J. and Choy, F. (1992), "Theoretical study of crack-induced eigenfrequence changes on beam structures", *J. Eng. Mech.*, ASCE, **118**(2), 384-396.

Ostachowicz, W.M. and Krawczuk, M. (1991), "Analysis of the effect of cracks on the natural frequencies of a cantilever beam", *J. Sound Vib.*, **150**, 191-201.

Qian, G.L., Gu, S.N. and Jiang, J.S. (1990), "The dynamic behaviour and crack detection of a beam with a crack", *J. Sound Vib.*, **138**, 233-243.

Rizos, R.F., Aspragotos, N. and Dimarogonas, A.D. (1990), "Identification of crack location and magnitude in a cantilever beam from the vibration modes", *J. Sound Vib.*, **138**, 381-388.

Specht, D.F. (1990), "Probabilistic neural networks", *Neural Networks*, **1**(3), 109-118.

Wu, J.R. and Li, Q.S. (2003), "Structural performance of multi-outrigger braced tall buildings", *The Structural Design of Tall Buildings*, **12**, 155-176.

Yun, C.B., Yi, J.H. and Bahng, E.Y. (2001), "Joint damage assessment of framed structures using a neural networks technique", *Eng. Struct.*, **23**(5), 425-435.

Zhou, X.Y. and Shen, P.S. (1997), "Study of damage assessment of concrete structures by strain model method", *Journal of Hunan University*, **24**(5), 71-74.